Spray impact on metallic meshes

C. Boscariol[1], D.J. Bouchard[2], M. Gibbons[2], M. Marengo[1], S. Chandra[2]
[1]Advanced Engineering Centre, School of Computing, Engineering and Mathematics,
University of Brighton, Lewes Rd., BN2 4GJ, Brighton, UK
[2]Department of Mechanical and Industrial Engineering
University of Toronto, Toronto, Canada
*Corresponding author: chandra@mie.utoronto.ca

Abstract
An experimental study was carried out to observe the impact of a full-cone water spray onto horizontal stainless steel meshes that were stretched over a ring to maintain uniform tension. The full-cone spray was generated using a portable spray can connected to a high-pressure compressed air cylinder, which provide a constant pressure of 760 kPa (110 psi). Three different meshes were used for the experiments, all having the same wire diameter (200 µm) but varying pore size (200, 400 and 800 µm). A high-resolution camera with a narrow depth of field was used to photograph droplets both above and below the plane of the wire mesh. Image analysis software was used to measure droplet size distributions from photographs. High speed video was taken of droplets impacting the mesh and penetrating through it. The mean droplet size was found to be in the range of 20-30 µm much smaller than the mesh pore dimensions. However, droplets landing on the 200 µm pore mesh were seen to coalesce with each other and form a liquid film suggested they adhered to the wires and blocked the pore apertures. In the case of the mesh with 400 µm pores water dripping from the wires was observed, so that the droplet size below the mesh was significantly larger than that of the impacting spray. Most droplets impacting the 800 µm mesh penetrated through the pores and no liquid layer was formed.

Keywords
Spray, mesh screen, porous surface, filtration.

Introduction

The impact of droplets on metallic wire meshes is seen in many applications: mesh screens are used to separate liquid from wet steam; polymer meshes are used to capture water droplets from coastal mists in arid areas; sprinklers are used to quench fires in electrical enclosures that have windows covered with wire mesh [1][2]. Droplet interaction with fibres is seen in natural phenomena such as the formation of dew on spider webs. The penetration of droplets into pores is observed during impact and infiltration of rain into soil [3], which is also related to analyses of soil erosion, nutrient and pollutant transport, water conservation and agricultural spray distribution [4]. Agrochemicals are typically distributed on plants by spraying them onto leaf surfaces into which they penetrate [5]. Porous structures can be used to enhance fuel vaporization by spraying fuel droplets on a porous coating on the piston crown [3]. In all these cases, it is important to know the mass flux and droplet sizes that either penetrate through the mesh or are captured by it.

Safavi et al. [1] performed an experimental and analytical study to analyse the capture of liquid droplets on fibrous filters, focusing on single droplet impact on a horizontal fibre. The impact of droplets on a thin wire may lead to two different outcomes: a high impact velocity causes the disintegration of the main droplet and the formation of smaller droplet whereas a low impact velocity leads to the formation of larger drops that drip from thick wires [1]. They compared experimental results with an analytical expression based on an energy balance, taking in account the effect of droplet eccentricity and wall adhesion in order to detect the threshold velocity at which droplets were capture by the wire. They obtained good agreement between experimental results and analytical predictions, and observed that a higher eccentricity of the droplet and a higher ratio of droplet radius to fiber radius, both lead to a lower threshold velocity for droplet capture. Kim et al. [6] performed a study on air and evaporative spray cooling of plain and microporous coated surfaces and determined heat transfer coefficients as a function of heat flux. They observed that spraying water droplets on the microporous coating surface enhanced heat removal due to capillary pumping through microporous cavities connected to each other. De Cock et al. [7] determined an optimum range of droplet sizes herbicide sprays using a modelling approach. They found out that a high control of deposition and an improved spray efficiency are obtained by using a droplet size in the range of 200 and 250 µm. Piroird et al. [8] analysed droplet impact on inclined fibres and observed that capture efficiency depends on the droplet velocity. At low impact speed, the droplet runs down the fiber, leaving a film behind, whereas at higher impact speed it crosses

the fiber and get deflected. Xu et al. [9] performed a study of impact of droplet on mesh membranes which are a functional material for gas-water or oil-water separation. They determined a critical impact velocity for which a daughter droplet will be generated below the pore and found a correlation between the number of mesh pores within drop project area and liquid penetration. Boscariol et al [10] performed a study on droplet impact on metallic meshes with a wide range of pore sizes. They identified several different outcomes, including deposition, penetration, imbibition and splashing. Introducing two new dimensionless parameters, M and γ, they managed to predict the outcomes of the impact for the given range of experimental parameters. Jakub et al. [11] simulated the deposition of a droplet on a fiber through a two-color lattice-Boltzmann method (LBM). They found different patterns depending of the fiber dimension and roughness and the droplet dimension. Jun Lee et al. [12] studied droplet impact on high-curvature structures at high temperature. Combining different liquid properties, droplet diameter and contact surface temperature, the impacting drops revealed three distinct impact regimes, which can be classified as tail, splash, and jumping modes.

The present paper present a preliminary experimental study to observe the impact of a full cone water spray onto horizontal stainless steel meshes. The first objective was to measure the rate of liquid penetration through meshes with different pore diameters.

Material and methods

Experiments were conducted using target surfaces selected from a set of stainless steel metal meshes used for filtration applications (McMaster-Carr, USA), with pore size D_p of 200, 400 and 800 µm respectively and wire diameter size D_w of 200 µm. Fig. 1 shows a sample of a scanning electron microscope (SEM) image of a mesh with pore dimension of 400 µm.

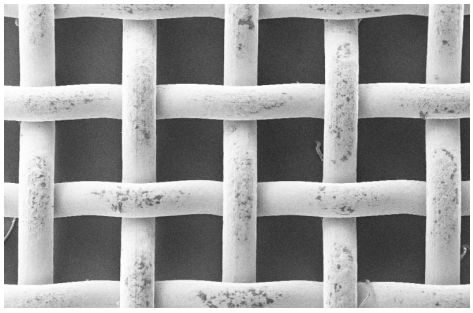

Fig. 1 SEM images of the stainless steel meshes sample with a pore diameter of 400 µm.

The spray can, (Model M, Sure Shot Milwaukee Sprayer, Menomonee Falls, WI, USA) clamped at a distance of 10 cm from the target surface, is connected to a high-pressure compressed air cylinder which provide a constant pressure of 760 kPa (110 psi). A spray diverter with a hole diameter of 5 mm, shown in Fig. 2, was mounted on the spray can to block all of the full-cone spray except for a small area in the centre of the spray diverter, limiting the mass flow hitting the target mesh.. The full-cone nozzle used on the spray can was model 305 (Sure Shot Milwaukee Sprayer, Menomonee Falls, WI, USA).

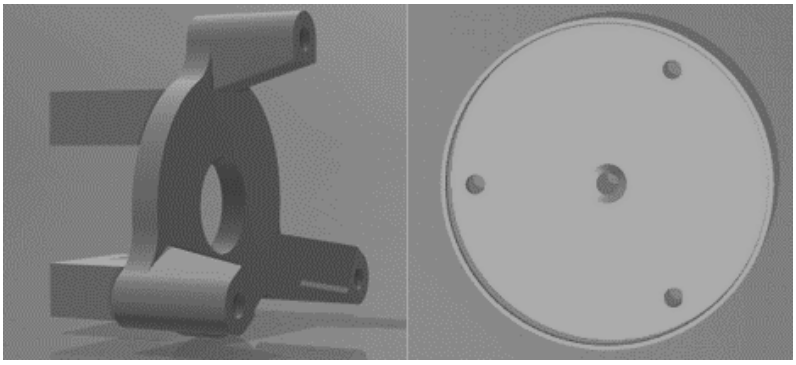

Fig. *2* Spray cone diverter: mounting bracket for attachment to spray can and bottom plate which attaches to the mounting bracket using three screws.

A portion of the mesh is suspended using a ring with a 20mm inner diameter. Two different angles of the camera are used to capture two different phenomena: the spray impacting on the mesh from the top view and the dripping regime from the bottom view. Fig. 3 shows a schematic of the experimental set up.

The droplet size distribution of the spray is characterised using a DropSizer (DMCH001, MazLite Inc, Toronto, Canada) that consists of a camera and a Class b laser with a wavelength of 905 nm pulsing at 100 ns. The depth of field was 0.23 mm, and the field of view is 3.20 x 2.40 mm. Fig. 4 shows one example of a frame captured by the DropSizer. The droplet size was calculated with a MATLAB code capable of extracting the average droplet diameter *d* and velocity v_i from different frames. The average droplet diameter is 25.45 μm and the average impact velocity is 2.8 m/s. Table 1 reports the data of mean velocity, mean droplet diameter and uncertainty for 4 different test spray cases.

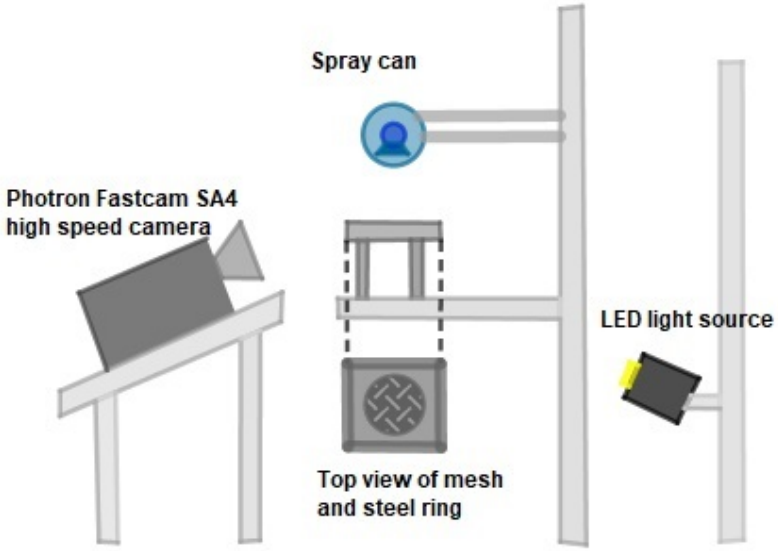

Fig. 3 Set-up schematic

Table 1 Spray characteristics

	Case 1	Case 2	Case 3	Case 4
v_i (m/s)	2.71	2.84	2.86	2.82
v_i sd 95%(m/s)	1.62	1.63	1.79	1.55
d (μm)	24.84	26.04	25.18	25.74
d sd 95% (μm)	26.85	23.09	28.45	24.74

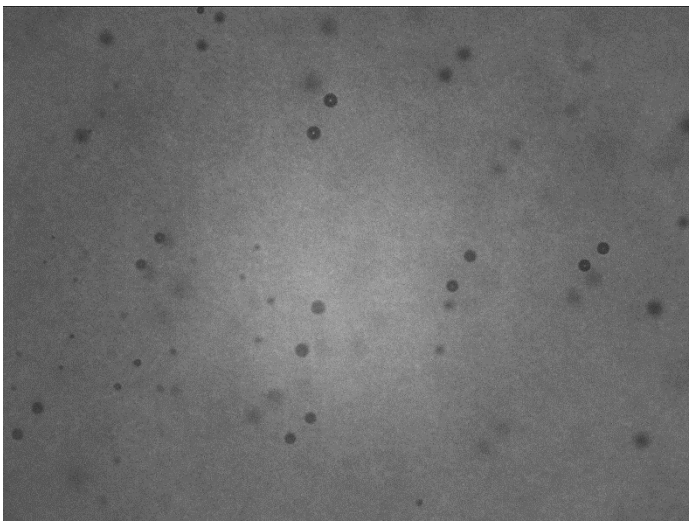

Fig. 4 Image captured by the DropSizer

Results and discussion

Spray impact on different meshes was observed for a duration of 4 seconds. Fig. 5 shows successive states during impact, viewed from above of the three different meshes. Time *t*=0 corresponded to the spray being turned on. For the case of the mesh with 200 μm pores liquid droplets began to collect on the surface of the mesh (see *t*=2 s) which blocked the pores and prevented water from penetrating, even though the average diameter the spray droplets was 25 μm. eventually a layer of water collected on the surface of the mesh. A similar effect is observable in the case of the 400 μm pore mesh though it takes longer for droplets to collect on the surface of the mesh. However, no liquid film is visible for the mesh with 800 μm pore size, suggesting that there is a threshold for the formation of liquid film, linked to the pore vs wire size for the case of low diameter/pore size ratio. Since a smaller fraction of the surface area consists of wires as pore size is increased, a larger number of droplets penetrate through the pores instead of hitting the wire. As the pore size is reduced to 200 or 400 μm the probability of a droplet of hitting the wire and being captured instead of penetrating into the pore is higher. Once multiple droplets have hit the same location and coalesced the liquid layer becomes thick enough to block a pore. Subsequent droplets then stay on the upper surface and form a continuous film.

The modified Reynolds and Weber numbers, based on the mesh pore diameter as a length scale are given by:

$$Re_p = \frac{\rho v_i d}{\mu} \times \frac{D_p}{d} \qquad We_p = \frac{\rho v_i^2 d}{\sigma} \times \frac{D_p}{d}$$

where v_i is the impact velocity of the spray,D_p the pore dimension, d the droplet diameter and ρ, μ, σ the density, viscosity and surface tension of water respectively. Using the same length scale, the dynamic and capillary pressures are

$$p_d = \rho v_i^2 \qquad p_c = \frac{2\sigma}{D_p}$$

For distilled water, the value for density, viscosity and surface tension are 996 kg/m^3 , 1 mPa s and 0.073N/m, respectively. Table 2 indicates the value of the fraction of open area for each mesh and the values of dimensionless number and pressures based on the average values of droplet diameter and impact velocities.

Table 2 Mesh fraction of open area and dimensionless number

Mesh pore size (μm)	% open area	Re_p	We_p	p_c [Pa]	p_d [Pa]
200	31	557.8	21.4	1460.0	1952.2
400	59	1115.5	42.8	730.0	1952.2
800	65	2231.0	85.6	365.0	1952.2

Fig. 6 shows the bottom view of the meshes during the same 4 second interval of spray impact in Figure 5. In the case of the 400 μm pore mesh droplets form on the underside, and then begin to drip off the wires. This effect is not seen for the 200 μm pore mesh where the water remained on the upper surface and there was no dripping, though wetting of the mesh could be seen. For the 800 μm pore mesh no dripping or wetting can be detected in such a short time interval sine most droplets passed through without hitting the wires.

Both 400 and 800μm pore meshes showed dripping if the spray was kept on for a sufficient period of time. Fig. 7 shows the bottom view of the meshes in the interval from 8 and 12s after the spray was turned on. The 400μm pore mesh showed the start of dripping earlier since there was a higher probability of droplets hitting the wires and forming a liquid film. Since the dripping takes place only after liquid film formation the onset of dripping appears later in the 800μm pore case. This suggests that a minimum number of droplets have to hit the wires for a liquid film to form. As the open area of the mesh is increased, a longer spraying time is necessary to form a film and for dripping to start. The rate of liquid penetration through the meshes was measured over a time interval of more than 100 s using an analytical scale (Mettler Toledo) placed under the meshes on which was placed a tray that captured all the liquid. Fig. 8 shows the liquid mass collected in four different cases: the red curve indicates the mass flow for the full cone spray, without any mesh while the black, green and blue curves show the liquid that penetrates for meshes with 800, 400 and 200 μm pore size, respectively. Virtually no penetration occurs through 200 μm pores,

and the mass flow rate increases with pore size. The mass penetrating the meshes does not increase monotonically with time but varies in steps, showing the effect of dripping in which large masses of liquid detach and fall.

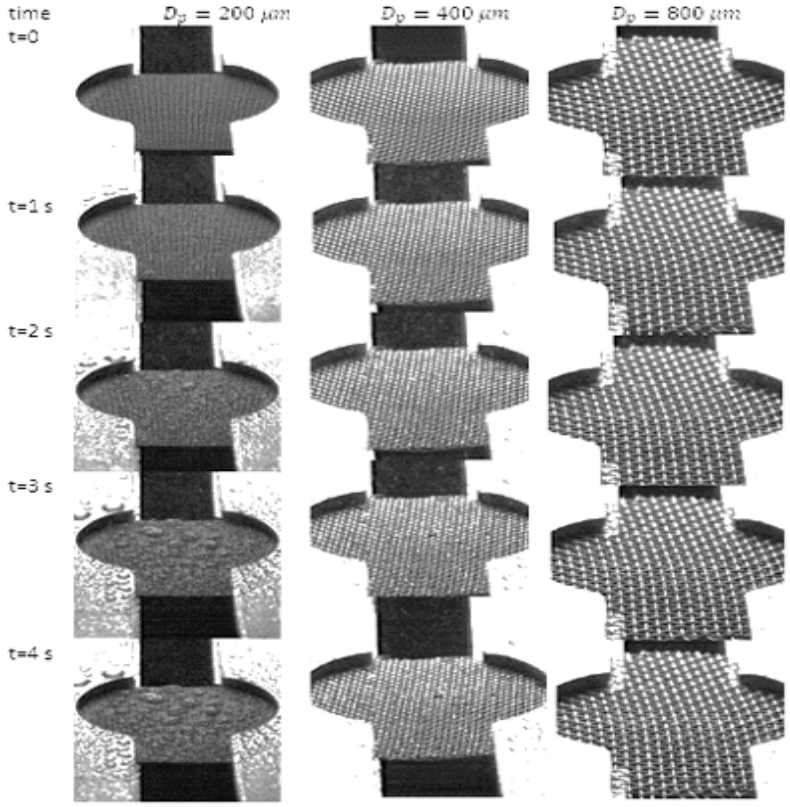

Fig. 5 Top view of the meshes during the first test in a time interval of 4 seconds. **The spray is turned on at t=0**

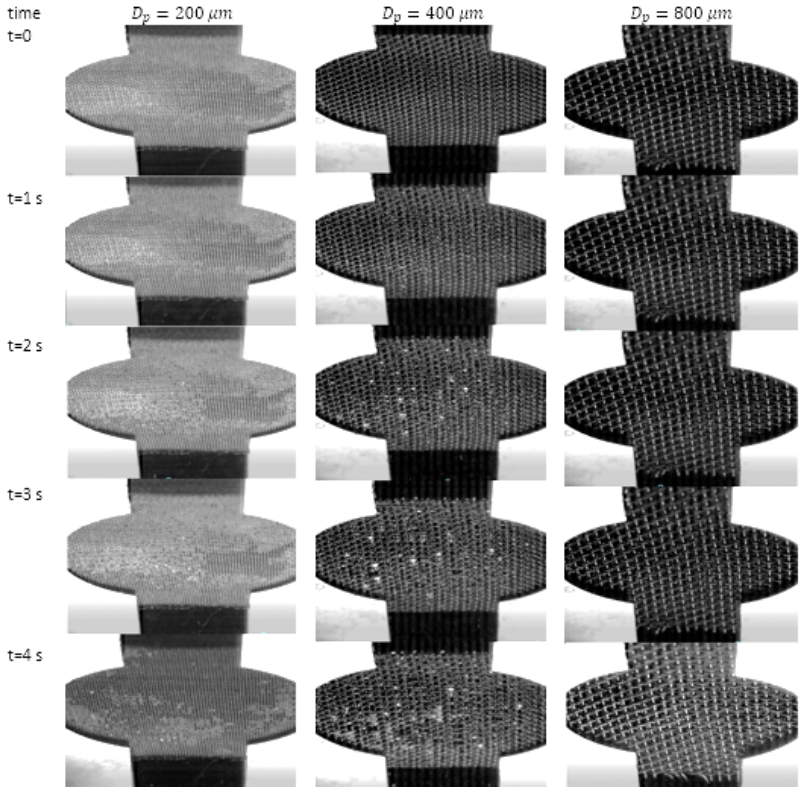

Figure 6. Bottom view of the meshes during the first test in a time interval of 4 seconds. The spray is turned on at t=0

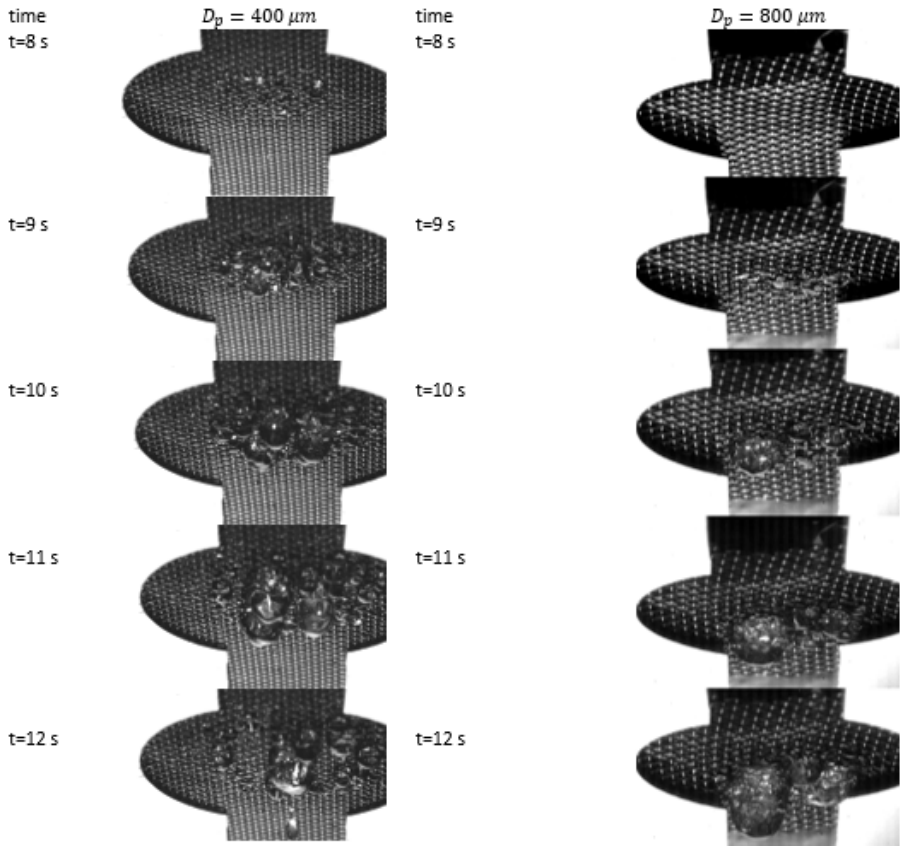

Figure 7. Dripping regime: bottom view of the meshes in the interval from 8 and 12s after the spray was turned on

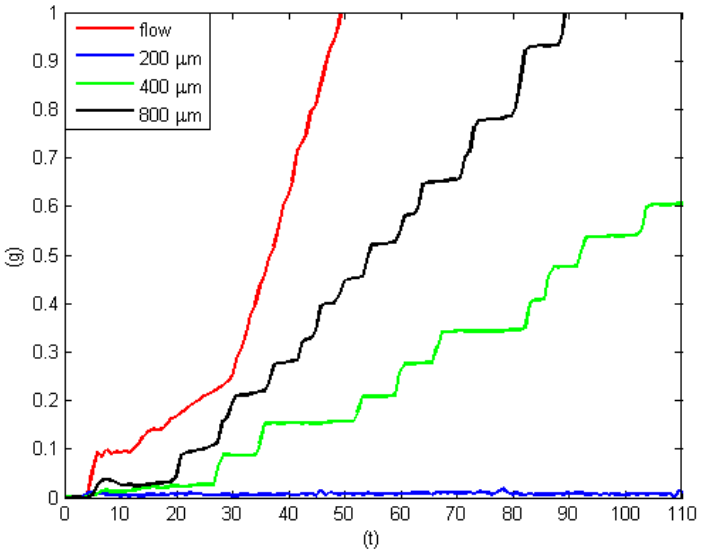

Figure 8 mass flow in measured over a time interval of more than 100 s using an analytical scale

Conclusions

A study was done on the impact of a full cone water spray on stainless steel meshes with 200, 400 and 800 µm pores. Despite the average droplet diameter (25 µm) being much smaller than the pore width for the finest mesh (200 µm), droplets sticks on wires and coalesce with each other to form a liquid film bridge, which grows and finally may block the pores and prevents further liquid droplets from penetrating. Considering a long spraying duration, it resulted that a liquid film can be formed also on the meshes with 400 and 800µm pore size, however, due to the larger dimension of the pores, the probability of the droplets hitting the wire is reduced, as the amount of liquid available to generate the liquid film bridge. Hence, the film will tend to collapse, and its rupture will lead to a dripping regime. It was observed that the dripping regimes occurs earlier in the case of pore size equal to 400µm with respect to the 800 µm mesh. This suggests that a minimum number of droplets landing on the wires is required to form the liquid film.

Acknowledgements
The stay of C. Boscariol and M. Marengo at the University of Toronto was financed by the EPSRC UK HyHP Project (EP/P013112/1).

Nomenclature

d	Droplet diameter [m]
D_p	Pore diameter [m]
D_w	Wire diameter [m]
p_c	Capillary pressure [Pa]
p_d	Dynamic pressure [Pa]
sd	Standard deviaiton
v_i	Impact velocity [m/s]
Re_p	Reynolds number
$\mathrm{We_p}$	Weber number
μ	Viscosity [Pa s]
ρ	Liquid density [kg/m^3]
σ	Surface tension [N/m]

References

[1] M. Safavi and S. S. Nourazar, “Experimental, analytical, and numerical study of droplet impact on a horizontal fiber,” *Int. J. Multiph. Flow*, 2018, in press, doi.org/10.1016/j.ijmultiphaseflow.2018.10.018
[2] Agranovski, I. E. and Braddock, R. D. (1998), Filtration of liquid aerosols on wettable fibrous filters. AIChE J., 44: 2775-2783. doi:10.1002/aic.690441218
[3] A. L. Yarin, “DROP IMPACT DYNAMICS: Splashing, Spreading, Receding, Bouncing…,” *Annu. Rev. Fluid Mech.*, vol. 38, no. 1, pp. 159–192, 2006.
[4] S. C. P. Carvalho, J. L. M. P. De Lima, and M. I. P. De Lima, “Using meshes to change the characteristics of simulated rainfall produced by spray nozzles Materials and methods,” vol. 2, no. 2, pp. 67–78, 2014.
[5] V. Bertola, “Some Applications of Controlled Drop Deposition on Solid Surfaces,” *Recent Patents Mech. Eng.*, vol. 1, no. 3, pp. 167–174, 2008.
[6] J. H. Kim, S. M. You, and S. U. S. Choi, “Evaporative spray cooling of plain and microporous coated surfaces,” *Int. J. Heat Mass Transf.*, vol. 47, no. 14–16, pp. 3307–3315, 2004.
[7] N. De Cock, M. Massinon, S. O. T. Salah, and F. Lebeau, “Investigation on optimal spray properties for ground based agricultural applications using deposition and retention models,” *Biosyst. Eng.*, vol. 162, pp. 99–111, 2017.
[8] K. Piroird, C. Clanet, É. Lorenceau, and D. Quéré, “Drops impacting inclined fibers,” *J. Colloid Interface Sci.*, vol. 334, no. 1, pp. 70–74, 2009.
[9] J. Xu, J. Xie, X. He, Y. Cheng, and Q. Liu, “Water drop impacts on a single-layer of mesh screen membrane: Effect of water hammer pressure and advancing contact angles,” *Exp. Therm. Fluid Sci.*, vol. 82, pp. 83–93, 2017.
[10] Boscariol, C., Chandra, S., Sarker, D. et al. " Drop impact onto attached metallic meshes: liquid penetration and spreading", Exp Fluids (2018) 59: 189. https://doi.org/10.1007/s00348-018-2640-y.
[11] J. M. Gac, A. Jackiewicz, Ł. Werner, and S. Jakubiak, “Consecutive filtration of solid particles and droplets in fibrous filters,” *Sep. Purif. Technol.*, vol. 170, pp. 234–240, 2016.
[12] S. J. Lee, J. H. Cha, K. M. Kim, and W. Choi, “International Journal of Heat and Mass Transfer Dynamics of drop impact on heated metal wires : Thermally induced transition from tail to splash to jumping modes,” *Int. J. Heat Mass Transf.*, vol. 131, pp. 226–236, 2019.